WORLD CONFERENCE ON TIMBER ENGINEERING 2025
BRISBANE, AUSTRALIA

Advancing Timber for the Future Built Environment

EXPERIMENTAL STUDY ON GLULAM POST-BEAM JOINTS WITH INCLINED SELF-TAPPING SCREWS UNDER CYCLIC LOAD

Shengdong Zhang[1], Zhiyang Lin[2] , Guangyu Gao[3]

ABSTRACT: To know the seismic performance of timber post-beam joints connected with inclined long self-tapping screws, an experimental study was carried out. 8 groups of specimens fabricated with nominal 13mm diameter WRT long self-tapping screws of SFS intec and Douglas fir GLULAM with 2 replicates in each group under cyclic load were tested. Impact factors such as number of screws, inclined angle, rows of screws, edge distance of screws, etc. were taken into account. The results show that the failure mode is tension failure of screws when the embedment length is long enough, the overall ductility coefficients of the joints are in the range of 1.70~2.52, the edge distance and the number of screws have impact on the capacities of the joints, but the inclined angles of the screws have no significant influence.

KEYWORDS: self-tapping screws, post-beam connections, cyclic load

1 – INTRODUCTION

A self-tapping screw (STS) is a hardened metal fastener equipped with screw threads and a drill point. It can self-tap internal threads that tightly match the screw threads in the drilled hole of the substrate material, thereby establishing a certain degree of mechanical interlocking between the screw threads and the substrate material extruded on both thread flanks and roots, achieving the connection of the metal fastener to the substrate material[1]. GLULAM post-beam joints connected with inclined long STS represent a relatively new form of timber structure joint.

Self-tapping screws have the characteristics of rapid penetration and excellent anchorage performance, which have a high axially load capacity if they are placed in wood. Blaß et al.[2] investigated timber-to-timber joints with inclined screws and believed a number of opportunities for joints with inclined screws. Ringhofer et al.[3] studied the effects of boundary conditions, loading speed, and burial angle of STS on the tensile load-bearing capacity in timber. Their experimental results indicate that excessively small margins will cause premature damage to the wood around the screw. Gaunt[4] found that geometric parameters such as pitch and thread shape of STS had no significant effect on the withdrawal resistance. Baek et al.[5] and Brandner[6] also reached similar conclusions. Gehri[7] conducted experimental research on the effect of screw spacing on the withdrawal capacity of screws anchored along the grain. Malo et al.[8] showed the promise of threaded rods (similar to STS) as fasteners to realize timber joints with considerable strength and stiffness. Fang et al.[9] studied the moment resisting performance of GLULAM post-beam connections with inclined STS. The experimental results indicated that this type of connection is characterized by a high moment resistance and rotation stiffness, but not very considerable deformability and energy dissipation capacity.

There are very few investigations on the seismic performance of timber post-beam joints connected with STS. Kasal et al.[10] studied the seismic performance of a timber frame with three-dimensional rigid connections with STS and found that post-beam joints with STS were not ductile enough and the frame failed in a brittle mode during the extreme event. Wang[11] conducted experimental investigations demonstrating that the failure modes of GLULAM post-beam joints with inclined STS correlate with the embedment length of STS and revealed that when the screw embedment length is sufficient, the joint failure mode manifests as screw tension failure; when the screw embedment length is inadequate, the joint fails by screw withdrawal failure.

This paper presents an experimental study on the behaviour of the GLULAM post-beam joints connected with inclined STS under cyclic load, considering the influence of factors such as number of screws, inclined angle, rows of screws, edge distance of screws, and the

[1] Shengdong Zhang, Department of Structural Engineering, Tongji University, 1239 Siping Road, Shanghai, 200092, P.R. China, Email: zhangsh_d@tongji.edu.cn.

[2] Zhiyang Lin, Department of Structural Engineering, Tongji University, 1239 Siping Road, Shanghai, 200092, P.R. China, Email: 372644241@qq.com

[3] Guangyu Gao, Department of Structural Engineering, Tongji University, 1239 Siping Road, Shanghai, 200092, P.R. China, Email: ok123now@163.com.

https://doi.org/10.52202/080513-0240

width of post-beam cross-sections on the long self-tapping screw connections in post-beam timber joints.

2 – EXPERIMENT DESCRIPTION

2.1 THE SAMPLES

The fully threaded 13 mm × 800 mm WRT type STS of SFS intec and GLULAM glued with same grade Douglas fir laminae were used in the post-beam joint specimens. The moisture content of the GLULAM was about 11.3%.

The cross sections of posts and beams were 225 mm × 300 mm and 225 mm × 500 mm, respectively. Segments of 1500mm in length from both posts and beams were selected for the study of the joints. The primary configuration of the screws was a single row of symmetrically arranged screws, with 2, 3, or 4 screws on each side. To investigate the influence of the number of screw rows on joint performance, specimens with double rows of symmetrically arranged screws was added with an edge distance of 120mm for the inner screws.

The post was placed horizontally and the beam vertically. The screws' edge distance parallel to the direction of beam sectional height denoted as e_h and the screws' edge distance parallel to the direction of beam sectional width denoted as e_w. Number of screws (2,3,4 in each side), inclined angles (0^o, 15^o, 30^o), rows of screws (single, double), edge distance of screws (20mm, 120mm), etc. are variables concerned in the study. 8 groups of specimens were tested under cyclic load with 2 replicates in each group.

Table 1 shows 8 different joints set for this experiment. The "J15-4s-120" means J for joint, 15 for 15^o inclined angle, 4 for total 4 screws (2 in one side), s for one row (d for two rows) in each side, 120 for 120 mm e_h (all others are 20 mm). B for 250 mm × 500 mm beam (all others are 225 mm × 500 mm). The loading mode is cyclic load. Fig. 1-Fig.4 shows the detailed configuration of each joint.

Table 1: Detailed information of all joints.

Joint	Single/double row setup	Edge distance e_h/e_w(mm)	Beam section size(mm)
J15-4s	Single	20/60	225 × 500
J15-6s	Single	20/60	225 × 500
J15-6d	Double	20/60	225 × 500
J15-8d	Double	20/60	225 × 500
J15-4s-B	Single	20/60	250 × 500
J15-4s-120	Single	120/60	225 × 500
J30-4s	Single	20/60	225 × 500
J0-4s	Single	20/60	225 × 500

Note: The section sizes of all posts are 225mm × 300mm, except 250mm × 300mm for J15-4s-B.

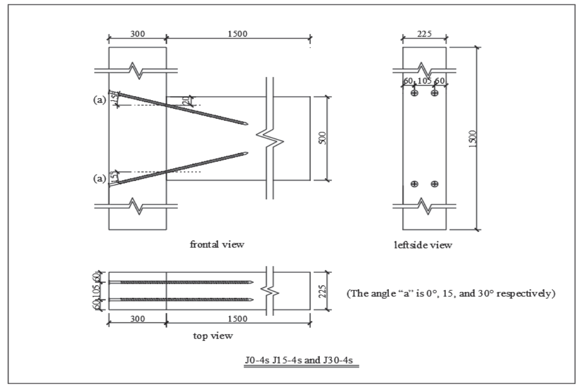

Figure 1. Detailed configuration of J0-4s, J15-4s and J30-4s.

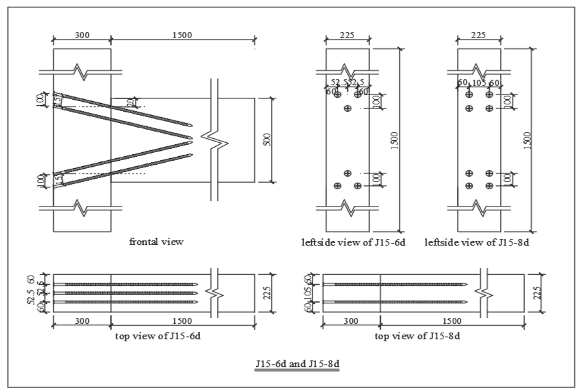

Figure 2. Detailed configuration of J15-6d and J15-8d

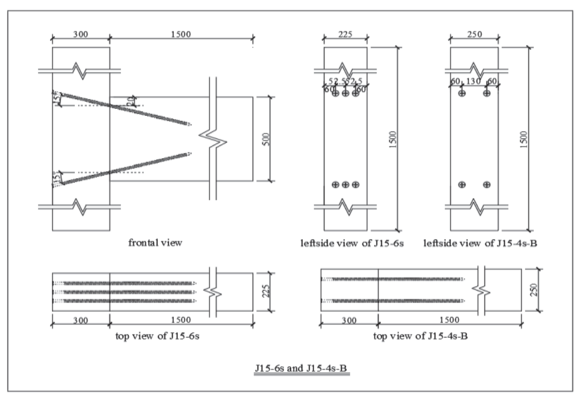

Figure 3. Detailed configuration of J15-6s and J15-4s-B

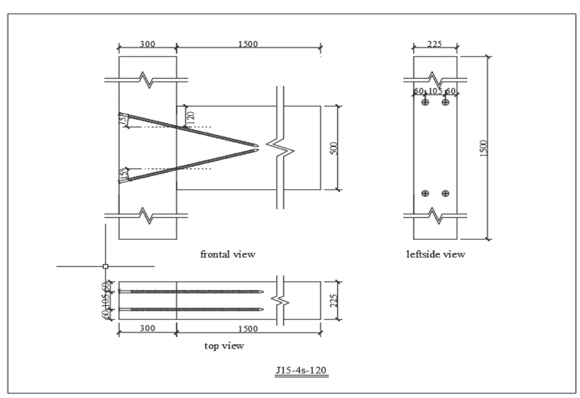

Figure 4. Detailed configuration of J15-4s-120.

https://doi.org/10.52202/080513-0240

2.2 THE TESTING PROCEDURE

The JAW-3002 electro-hydraulic servo loading system was used with displacement- controlled loading following the ASTM E2016[12] cyclic loading protocol as shown in Fig. 5. According to the experimental data from Wang[11], the ultimate displacement for this test was estimated to be 50mm. In the first phase, cyclic loading was conducted at 1.25%, 2.5%, 5%, 7.5%, and 10% of the displacement, with the loading rate controlled within 7.5mm/min. In the second phase, the loading amplitude was performed in three cycles at 15%, 20%, 40%, 60%, 80%, and 100% of the ultimate displacement, with the loading rate ranging between 10-30mm/min. If no failure occurred at this stage, the loading amplitude would be incrementally increased to 20% for further loading, with the number of cycles remaining at three times. To thoroughly investigate the symmetry of the joint under cyclic load, the test continued even after unilateral failure occurred, until the load on the opposite side dropped to 50% of the ultimate load. Fig. 6 shows the test set up.

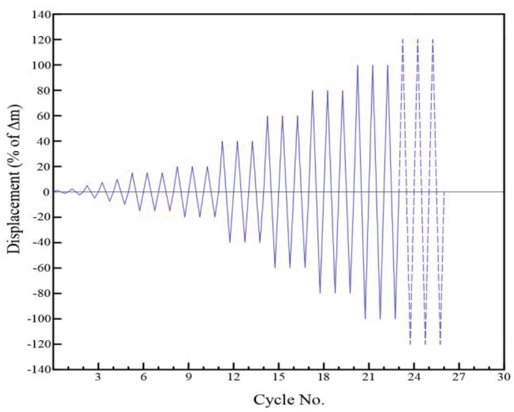

Figure 5. The cyclic loading protocol

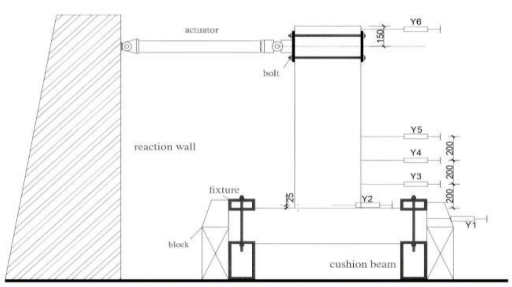

Figure 6. The test set up

3 – TEST RESULTS

3.1 FAILURE MODE

The failure mode of all specimens is tension failure of screws since all screws have long embedment length.

Taking the loading to failure process of J15-4s-1 post-beam joint specimen as an example. In the initial loading phase, when the reciprocating displacement did not exceed 10mm (20%), both the timber and screws were in an elastic state, and there was no significant change in the appearance of the joint. When the displacement was first loaded to $+20mm_{(1)}$ (the subscript number represents the cycle number of displacement) (40%), a small gap appeared at the post-beam interface. When the displacement reached $-30_{(1)}$ mm (60%), the joint produced a significant shifting sound, and a crack parallel to the grain appeared along the tension side of the beam end. When the displacement was loaded to 30-40mm, the load-displacement curve gradually flattened, indicating that the screws had entered the plastic phase. As the displacement approached $+40_{(1)}$ mm (80%), the joint emitted a loud noise, and two screws on one side broke simultaneously. As the test continued, the complete fracture of screws on one side did not affect the load-bearing performance of the other side. In the range of 0 to -40mm, the load gradually increased, reaching the level before the screws broke, and finally, at $-40_{(2)}$ mm (80%), the screws on the other side also completely fractured. The GLULAM post and beam showed good integrity after the entire loading process.

Fig. 7 shows the failure mode of joint J15-4s-1 during this loading process. The failure modes of other joints are shown in Fig. 8-Fig. 14.

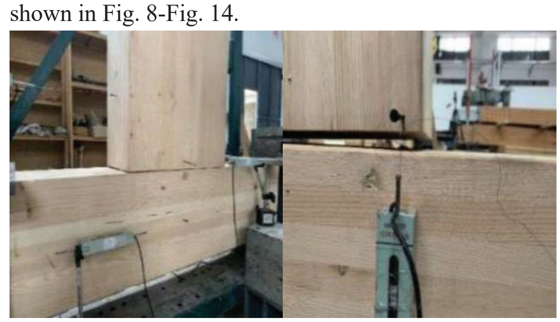

Figure 7. Tension failure of J15-4s

Figure 8. Tension failure of J15-6s

Figure 9. Tension failure of J15-6d

Figure 10. Tension failure of J15-8d

Figure 11. Tension failure of J15-4s-B

Figure 12. Tension failure of J15-4s-120

Figure 13. Tension failure of J0-4s

Figure 14. Tension failure of J30-4s

Except for the J30-4s joint, screw failures in all other joints occurred at the interface of the post and the beam, and none of them experienced withdrawal failure. In the J30-4s joint group, screw fractures occurred with a bit distance to the post-beam interface. Upon sectioning J30-4s with a cutting machine, it was observed that the screws were well-embedded in the GLULAM without any signs of scraping. Near the interface, the GLULAM showed plastic embedment deformation due to the screws' bending. The screws fractured within this zone, which is shown in Fig. 14.

3.2 LOAD-DISPLACEMENT CURVES

The load-displacement curve is a comprehensive reflection of the seismic performance of the specimen. Based on the horizontal load measured by the hydraulic servo horizontal brake and the lateral displacement measured by various displacement sensors, the moment-rotation hysteresis curves of each group of specimens can be obtained, as shown in Fig. 15-Fig. 22.

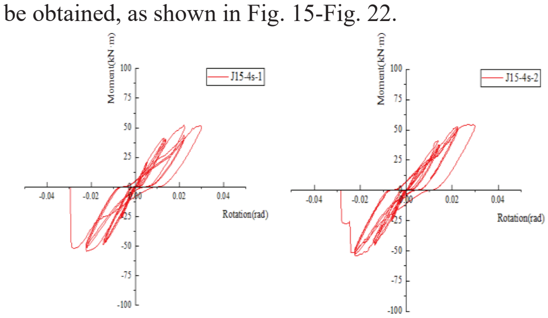

Figure 15. Moment-rotation hysteresis curves of J15-4s

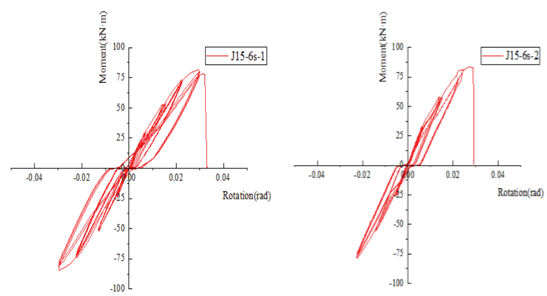

Figure 16. Moment-rotation hysteresis curves of J15-6s

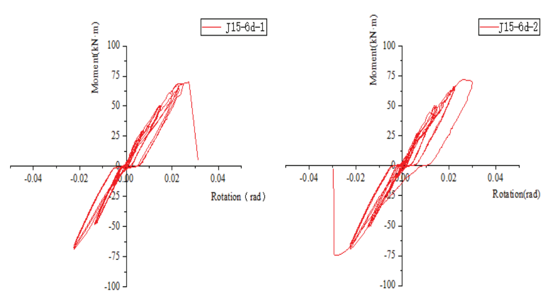

Figure 17. Moment-rotation hysteresis curves of J15-6d

https://doi.org/10.52202/080513-0240

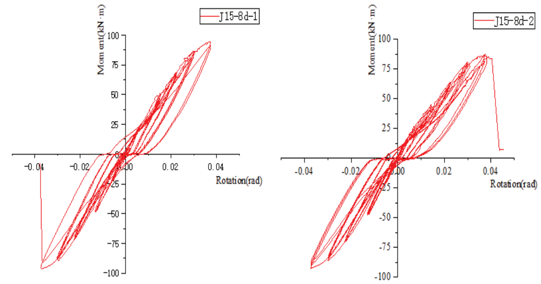

Figure 18. Moment-rotation hysteresis curves of J15-8d

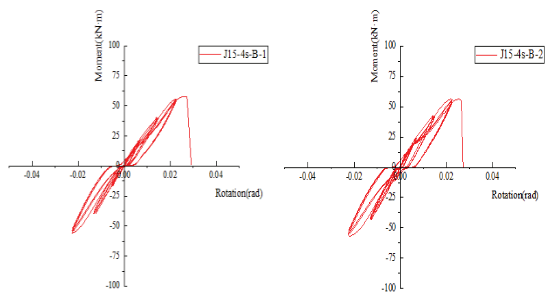

Figure 19. Moment-rotation hysteresis curves of J15-4s-B

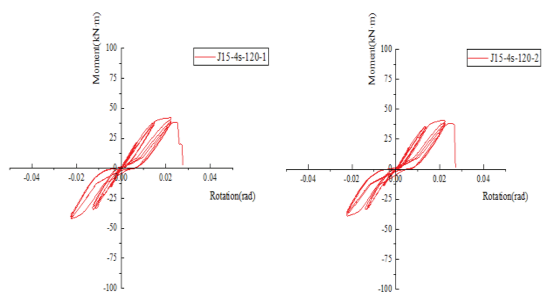

Figure 20. Moment-rotation hysteresis curves of J15-4s-120

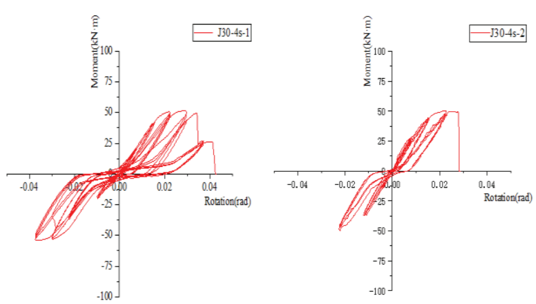

Figure 21. Moment-rotation hysteresis curves of J30-4s

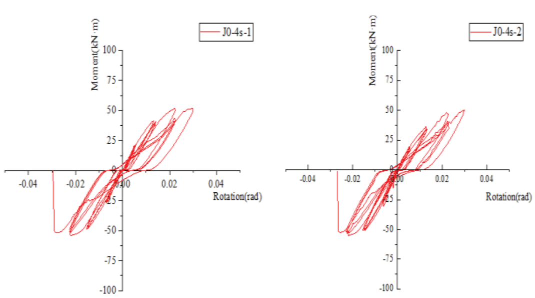

Figure 22. Moment-rotation hysteresis curves of J0-4s

The hysteresis curves of the STS post-beam joints studied in this experimental study generally exhibit an inverted "S" shape, with the loading and unloading conditions being essentially the same, demonstrating significant symmetry.

Comparing the J0-4s, J15-4s, and J30-4s joint groups, it can be observed that the inclined angles has insignificant impact on the capacity but those of 30° show better deformability than those of 0° and 15°.

Comparing the J15-4s with the J15-4s-B joint groups, it is evident that the larger the cross-sectional width of the GLULAM in the post and beam, the "steeper" the hysteresis curve of the joint.

Comparing the J15-4s with the J15-4s-120 joint groups, it can be seen that an increase in the edge distance of the long STS leads to a larger loop area in the hysteresis curve, but a significant reduction in the load-bearing capacity of the joint; similar observations are noted in the J15-6s and J15-6d joint groups.

The skeleton curve is the envelope line formed by connecting the maximum load points at each displacement control level during cyclic loading tests, which reflects the strength, stiffness, and displacement changes of the joint at different loading stages. The skeleton curve is an important method for evaluating the seismic performance of joints.

Based on the data from the hysteresis curves, the peak loads of the two specimens in each joint group at each displacement loading level were averaged, and the corresponding points were connected to obtain eight skeleton curves, as shown in the Fig. 23.

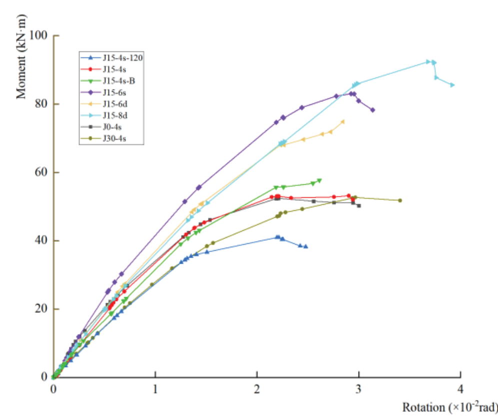

Figure 23. Skeleton curves of each group (averaged)

It can be observed the effects of screw embedment angle, post-beam cross-sectional width, screw edge distance and row configuration on the skeleton curves are shown in the Fig. 24-Fig. 27.

Fig. 24 shows that the embedment angle of screws does not significantly influence the bending capacity of the joints. The curve of 15 degree is very close to the curve of

0 degree but the curve of 30 degree shows lower stiffness and higher deformability than the other two. Fig. 25 shows that as the cross-sectional width increases, the bending capacity of the joints experiences a slight improvement. Fig. 26 shows that the capacity and ductility of the joint decreases with increasing screw edge distance. Fig. 27 shows that for the specimens with same number of screws in each side the two-row screw configuration does not exhibit good ductility (we expected) compared to the single-row screw configuration. Additionally, the load-bearing capacity of the joint was observed to increase significantly with a higher number of screws in same rows.

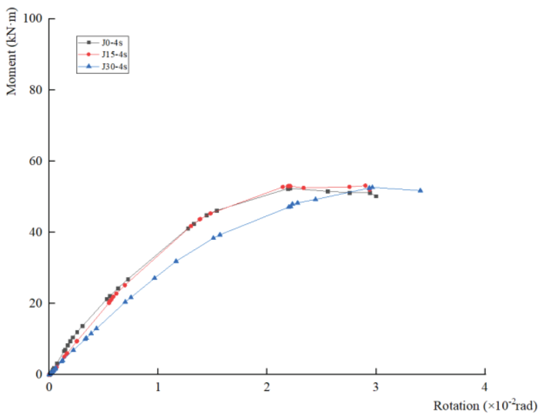

Figure 24. The influence of screw embedding angle

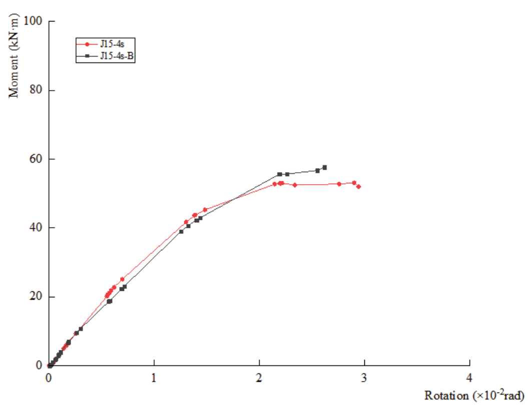

Figure 25. The influence of post and beam section width

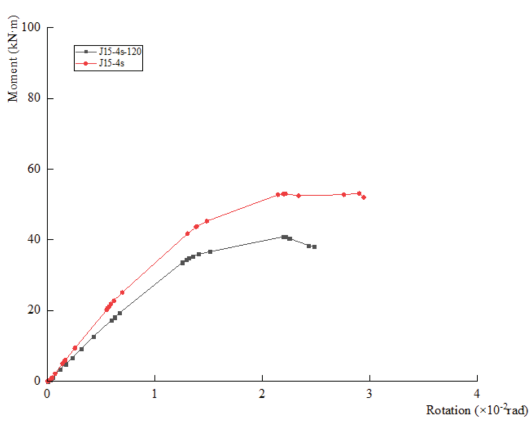

Figure 26. The influence of screw edge distance

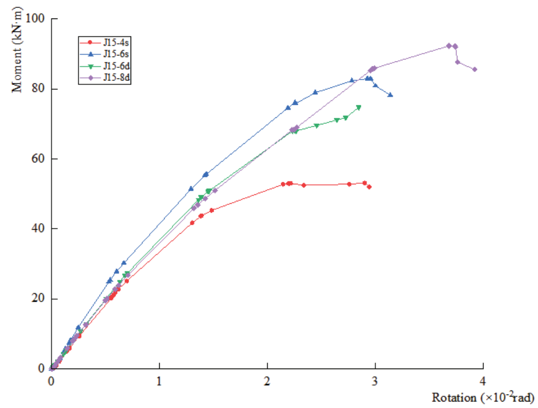

Figure 27. The influence of rows/number of screws

3.3 DUCTILITY PERFORMANCE

Ductility performance reflects the deformation capacity of a structure from the point it reaches its maximum load-bearing capacity until complete failure. The ductility coefficient μ is commonly used to represent the ductility performance of a joint, and it is defined as the ratio of the ultimate rotation angle (θ_u) to the yield rotation angle(θ_{yield}). In this study, the Idealized Elastic-Plastic Energy Equivalent (EEEP) method introduced in ASTM E2126 was used to analyze and calculate the backbone curve to determine the relevant parameters. The peak moment (M_{peak}) is the maximum moment value reached on the backbone curve of the joint, and the peak rotation angle (θ_u) is the rotation angle corresponding to the peak moment. The ultimate moment (M_u) is taken as the moment value corresponding to the maximum rotation angle recorded on the backbone curve; however, if this value is less than 0.8Mpeak, then 0.8Mpeak is used instead. θ_u is the rotation angle corresponding to the ultimate moment (M_u). The yield moment (M_{yield}) is calculated using Equation (1):

$$M_{yield} = \left(\theta_u - \sqrt{\theta_u^2 - \frac{2A}{K_e}} \right) K_e \qquad (1)$$

Where A is the area under the skeleton curve from the origin to the ultimate displacement, and the elastic stiffness (K_e) is the secant stiffness corresponding to 0.4 times the maximum moment point (M_{peak}).

Based on the 8 skeleton curves of the self-tapping screw post-beam joints and the calculation method described above, the mechanical performance indicators of the long STS post-beam joints are summarized in Table 2.

Table 2: Mechanical performance indicators of each joint

Joint	M_{yield}	θ_{yield}	M_{peak}	M_u	θ_u	μ
J15-4s	48.90	1.32	53.14	52.00	2.94	2.23
J15-6s	73.05	1.66	82.99	78.22	3.14	1.88
J15-6d	64.19	1.67	74.80	74.80	2.84	1.70
J15-8d	80.77	2.25	92.34	85.55	3.92	1.74

https://doi.org/10.52202/080513-0240

J15-4s-B	51.92	1.61	57.67	57.67	2.61	1.63
J15-4s-120	37.53	1.29	40.97	38.22	2.48	1.93
J30-4s	47.26	1.62	52.64	51.74	3.41	2.10
J0-4s	47.80	1.19	52.37	50.22	3.00	2.52

The ductility coefficients of long STS post-beam joints are in the range of 1.70~2.52. For this kind of joint configuration, the ductility of the joint depends on the deformability of the screws. The reason of the ductility of the joints are not good enough is that the deformabilities of the screws are not very high and the elongations of the screws do not happen in full lengths but in very small part around the post and beam interface.

From the data of J0-4s, J15-4s, and J30-4s, it can be observed that as the embedment angle of the screws in the GLULAM gradually increases, the elastic stiffness gradually decreases, and the ductility coefficient also decreases. However, the change in angle has little effect on the peak moment of the joints, which are 52.37 kN·m, 53.14 kN·m, and 52.64 kN·m, respectively.

From the data of J15-4s and J15-6s, it can be observed that the ductility of the joints decreases as the number of screws increases. The peak moment increases almost linearly with the number of screws.

From the data of J15-4s and J15-4s-120, it is evident that as the edge distance of the screws increases, the peak moment, elastic stiffness and ductility coefficient of the joints all decrease. This suggests that increasing the edge distance of the screws gradually reduces their utilization efficiency, making it an uneconomical configuration.

From the data of J15-4s and J15-4s-B, it can be observed that an increase in the cross-sectional width of the GLULAM post-beam results in a slight increase in the peak moment of the joints, which are 53.14 kN·m and 57.67 kN·m, respectively.

4 – CONCLUSIONS AND RECOMMENDATIONS

This paper presents the results of cyclic loading tests on GLULAM post-beam joints connected with long STS. Under the conditions of sufficient embedment length of the STS and unchanged beam cross-sectional height, the ultimate load-bearing capacity and ductility of the joints were comprehensively considered in terms of number of screws, inclined angle, rows of screws, edge distance of screws, etc. The main conclusions of this study are as follows:

(1) After analyzing the experimental data and failure modes of each joint group, it was found that for timber post-beam joints connected with STS, the failure mode is tension failure of screws if the embedment length is long enough. The joints do not show good ductility. 30^{o} angle shows better deformability, possibly due to local wood embedment failure, which increases the length of STS that can freely elongate. The deformability of this kind of joint is mainly due to the deformability of screws.

(2) The number of screws and the edge distance have a significant impact on the joint's capacity. The more screws and the smaller the edge distance, the greater the flexural capacity of the joints. The inclined angles have insignificant impact on the capacity. The edge distance of the screws and the cross-sectional width of the post-beam have a critical impact on ductility; the larger the edge distance and cross-sectional width, the worse the ductility performance of the joints. Two rows of screws arrangement do not show better ductility (we expected) than one row.

(3) Each group of joints with different configurations set up in this experimental study had only two specimens. The results may be biased due to the variability in the properties of the GLULAM or the STS. The study only established two cases of cross-sectional widths, 225mm and 250mm, and the variation in some parameters of the joints was small, making it difficult to clearly derive the performance change patterns of the joints due to parameter changes. It is recommended that future research work increase the number of specimens and add numerical analysis. Further research on how to improve the ductility of post-beam joints should be carried out in the future.

5– REFERENCES

[1] L. Fang. “Mechanical Performance of GLULAM Beam-column Moment-resisting Connection with Self-tapping Screws.” PhD thesis, Tongji University, Shanghai, China (in Chinese), 2022.

[2] H.J. Blaß, I.Bejtka. “Screws with continuous threads in timber connections.” In: RILEM Symposium: Joints in Timber Structures, Proceedings PRO vol. 22, 2001. Stuttgart, Germany.

[3] A. Ringhofer, R. Brandner, and G. Schickhofer. “A universal approach for withdrawal properties of self-tapping screws in solid timber and laminated timber products.” In: Proceedings of The 2nd Inter-Meeting, Š ibenik: Croatia, 2015.

[4] D. Gaunt. “The effect of thread geometry on screw withdrawal strength.” In: NZ Timber Des J, vol. 6(3), 1997. pp. 12-20.

[5] H.S. Baek, H. Morita, A.Shiiba et al. “Influence of shape factors of wood screw on withdrawal performance.” In: Proceedings of WCTE 2012 – World Conference on Timber Engineering. Auckland:New Zealand, 2012.

[6] R. Brandner. “Properties of axially loaded self-tapping screws with focus on application in hardwood.” In: Wood Material Science & Engineering, vol. 14(5), 2019. pp. 254-268.

[7] E. Gehri, “Influence of fasteners spacings on joint performance–Experimental Results and Codification” In: Proceedings of the 42nd CIB-W18 meeting. Dübendorf: Switzerland, 2009.

[8] K.A. Malo, H. Stamatopoulos. “Connections with threaded rods in moment resisting frames.” In: Proceedings of WCTE 2016 – World Conference on Timber Engineering. Vienna: Austria, 2016. 74.

[9] L. Fang, W. Qu, S. Zhang. “Rotational behavior of GLULAM moment-resisting connections with long self-tapping screws.” In: Construction and Building Materials, vol. 324, 2022.

[10] B. Kasal, P. Guindos, T. Polocoser et al. “Heavy laminated timber frames with rigid three-dimensional beam-to-column connections.” In: Journal of Performance of Constructed Facilities, vol. 28(6), 2014.

[11] L. Wang, “Seismic Performance of Post and Beam Timber Connections with Long Self-tapping Screws.” M.S. thesis, Tongji University, Shanghai, China (in Chinese), 2018.

[12] American Society for Testing and Materials (ASTM). Standard test methods for cyclic (reversed) load test for shear resistance of vertical elements of the lateral force resisting systems for buildings. 2011.

https://doi.org/10.52202/080513-0240